Dataset overview.

Layered earth inversion of the Lower Macquarie River TEMPEST AEM Survey, NSW, 2007.

1.0 Overview

This product contains three airborne geophysical datasets:

- the final geophysical inversion of the Lower Macquarie River TEMPEST airborne electromagnetic (AEM) survey data using a layered earth inversion algorithm developed by Geoscience Australia (GA-LEI);
- an airborne magnetic survey and;
- a digital elevation model (DEM).

These data include enhancements of previously available datasets, using more recent geophysical processing software advances.

The TEMPEST time domain airborne electromagnetic (AEM) survey was flown in 2007 by Fugro Airborne Surveys (FAS) over the Lower Macquarie River catchment, northwest of Dubbo in the central west New South Wales, Australia (figure 1 and figure 2). The survey was commissioned by the Australian Government Department of Agriculture, Fisheries and Forestry through the Australian Bureau of Agricultural and Resource Economics and Sciences (ABARES, formerly Bureau of Rural Sciences) and funded under the National Action Plan for Salinity and Water Quality. Geoscience Australia (GA) provided several geophysical services in relation to the survey including survey planning, technical system selection, data quality control and layer earth inversion of the resultant data.

Figure 3 below gives a graphical overview of the directory structure of this data product.

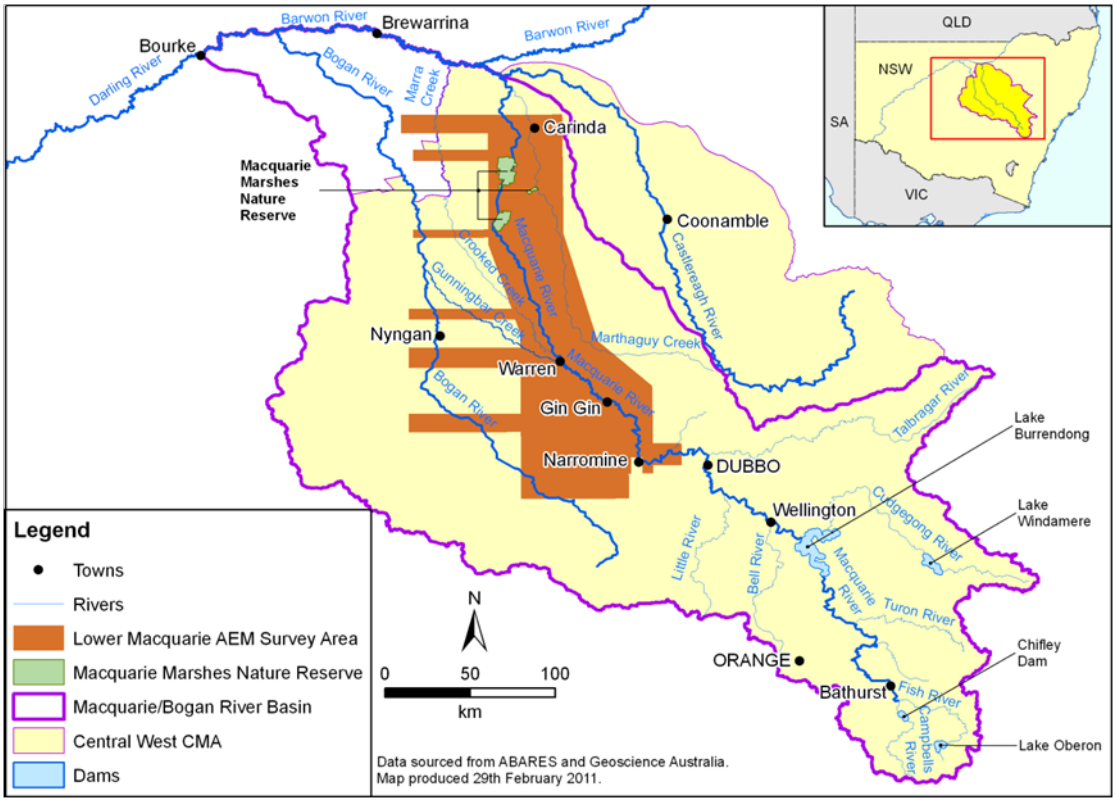

Figure 1: Location of the Lower Macquarie River AEM survey area

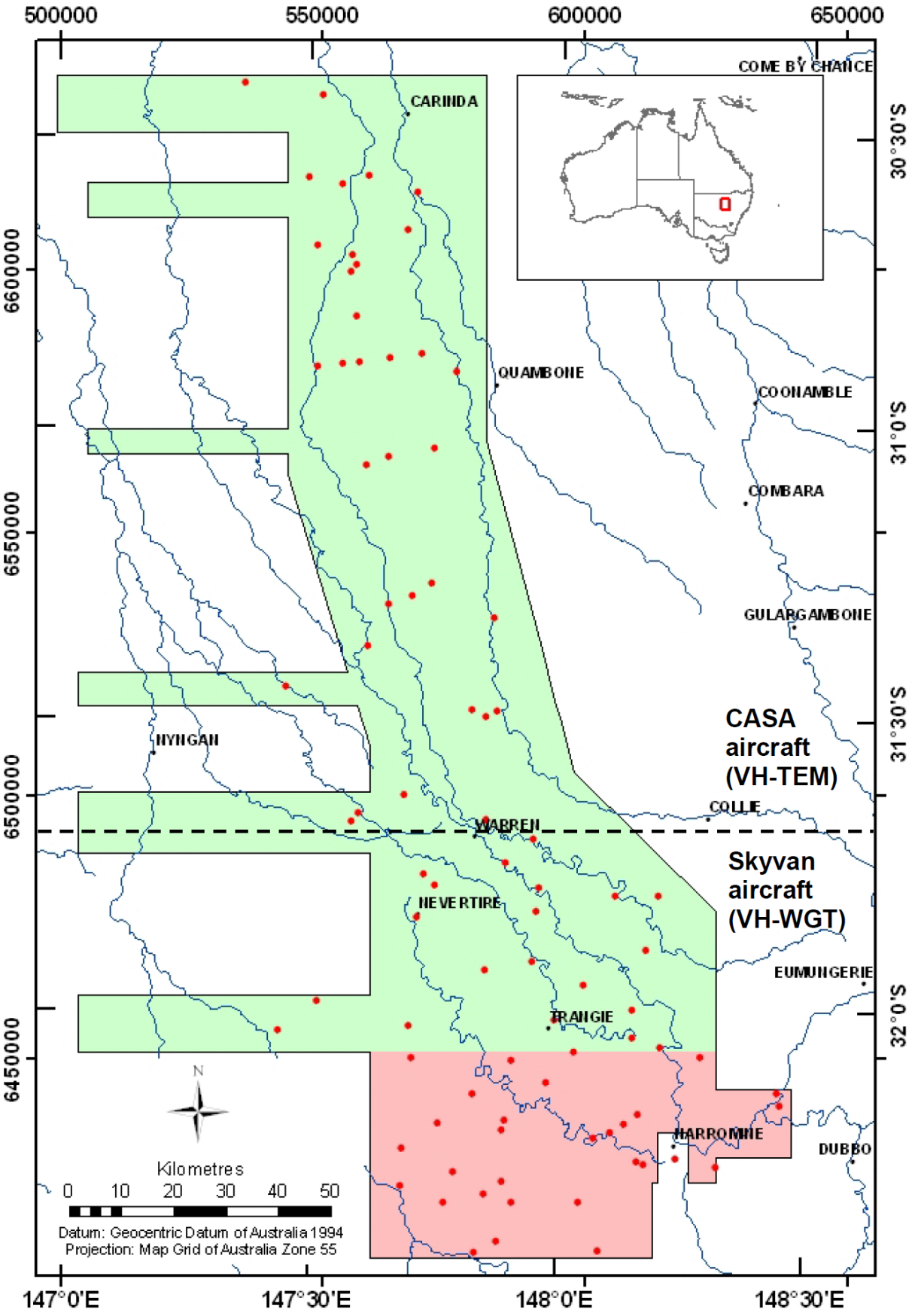

Figure 2: **Location of the Lower Macquarie River AEM survey area and downhole conductivity logs (red dots). The northern area (green) was flown on east-west lines and the southern area (pink) was flown on north-south lines. The dashed line is along flight line 24810.**

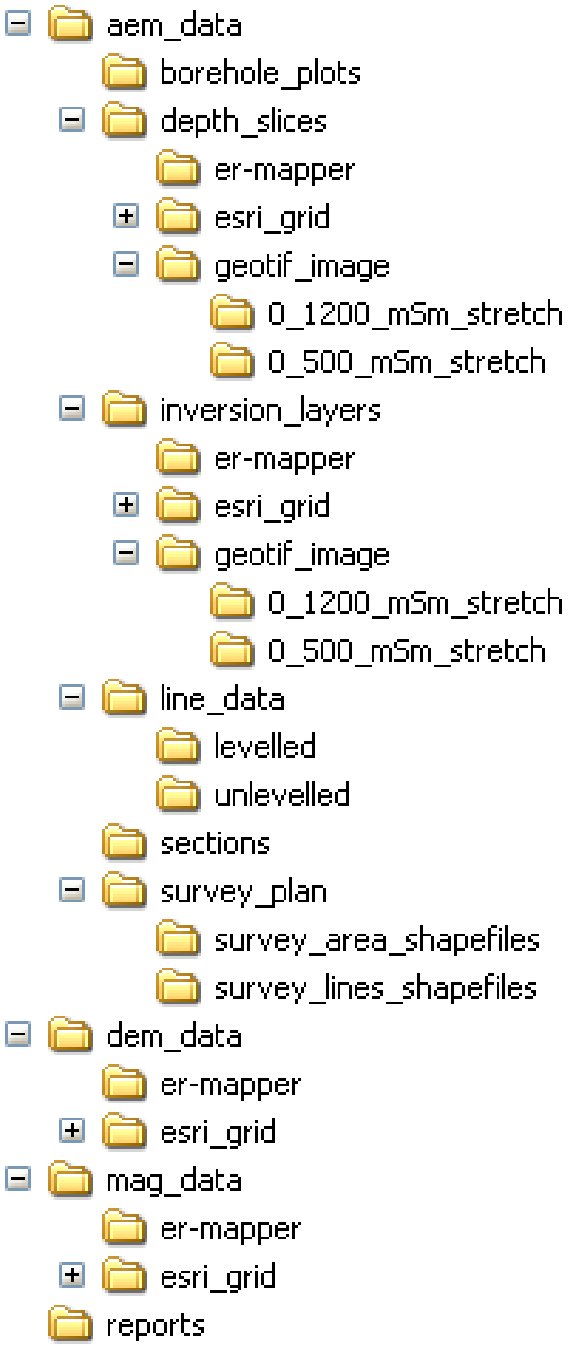

Figure 3: Graphical overview of the directory structure of this data product

The following sections describe the key datasets in this data product.

Appendix 1 gives a detailed list of the contents of each directory and the dataset components.

2.0 AEM data

The AEM survey data includes the final geophysical inversion of the Lower Macquarie River TEMPEST airborne electromagnetic (AEM) survey data using a layered earth inversion algorithm developed by Geoscience Australia (GA-LEI). The GA-LEI AEM data are derived from the 'Lower Macquarie River TEMPEST AEM Survey, NSW, 2007 Final Data', available as Geoscience Australia product 67211 (GeoCat #67211). The GA-LEI algorithm has been demonstrated to generate more accurate conductivity predictions than the conductivity depth transform predictions available in GeoCat #67211 for other similar TEMPEST surveys.

The AEM datasets are:

- line (point located) data of layer conductivity, depths below ground level, and thicknesses. These are the primary data output of the GA-LEI inversion process (sub-folder: line_data)
- grids of the conductivity model layers interpolated from the inversion line data; the layers are relative to ground surface (sub-folder: inversion_layers)
- grids of conductivity depth slices of regular thicknesses generated from the layers; the depth slices are relative to natural surface (sub-folder: depth_slices)
- vertical conductivity–depth sections along flight lines (sub-folder: sections); these are graphical representations of the estimated conductivity in a vertical slice along the line of best fit passing through the flight line. These sections were produced for each flight line in the AEM survey.
- AEM survey outline and flight line vector GIS data (sub-folder: survey_plan); these are the outline of the Lower Macquarie River TEMPEST AEM survey area and the actual flight line path flown in the survey, as a line dataset.
- borehole comparison logs (sub-folder: borehole_plots); these plot the profile by depth of independent measurements of conductivity acquired down boreholes against the AEM inverted conductivity. These are available for each of the 83 bores inside the survey area for which downhole conductivity logs were acquired.

2.1 Line data (sub-folder: line_data)

The results of the GA LEI are stored in a point located (or line) format, in an ASCII file formatted with space-delimited columns. Each record represents one sample along a flight line, which records the conductivity values for the modelled layers. A comprehensive header file is associated with the file, which describes the data and the numeric format of each column in the file. Every fifth survey sample or 550,541 samples in total were inverted.

Two sets of line data files are supplied:

Sub-folder line_data\unlevelled

This dataset contains the output on the 25 layer GA-LEI inversion procedure, without any post inversion processing.

The results of the GA LEI are stored in a point located (or line) format, in an ASCII file formatted with space-delimited columns (inversion.output.dat). Each record represents one sample along a flight line. A comprehensive header file (inversion.output.hdr) is associated with the file, which describes the data and the numeric format of each column in the file.

Sub-folder: line_data\levelled

This dataset contains the outcome of the post inversion processing of the 25 layer GA-LEI inversion procedure. This is the dataset from which the gridded AEM datasets are derived.

Details of the levelling and micro levelling corrections applied are described in Brodie and Fisher (2008) and summarised here:

- Levelling corrections to correct the mismatch in the in the conductivity values on either side of the join between the lines flown by VH-WGT and VH-TEM
- Micro-levelling to reduce the effect of artefacts aligned in the flight line direction

Gridding and micro-levelling operations were carried out using the Intrepid Software package (v4.1 Release Build 125).

The output of the levelled and micro-levelled GA-LEI AEM inversion data are stored in an Intrepid database file set. The point located data are stored in an ASCII file (inversion.output.levelled.dat) formatted with space-delimited columns. A comprehensive header file (inversion.output.levelled.ddf) is associated with the file, which describes the data and the numeric format of each column in the file.

2.2 Layer conductivity grids (sub-folder: inversion_layers)

The layer conductivity grids represent the conductivity in siemens per metre (S/m) of each layer of the 25 layer conductivity model. The data were gridded to a square 75 m cell size from the micro-levelled point located data using minimum curvature gridding. There are always 25 layers in the model and the thickness of each layer is constant over the whole survey area. The layer thicknesses and depth extents are shown in Table 1. All depths are relative to the natural surface.

Table 1 Conductivity inversion model layer thicknesses and depths.

Layer number	Thickness (m)	Depth to top (m)	Depth to bottom (m)
1	2.00	0.00	2.00
2	2.20	2.00	4.20
3	2.42	4.20	6.62
4	2.66	6.62	9.28
5	2.93	9.28	12.21
6	3.22	12.21	15.43
7	3.54	15.43	18.97
8	3.90	18.97	22.87
9	4.29	22.87	27.16
10	4.72	27.16	31.87
11	5.19	31.87	37.06
12	5.71	37.06	42.77
13	6.28	42.77	49.05
14	6.90	49.05	55.95
15	7.59	55.95	63.54
16	8.35	63.54	71.90
17	9.19	71.90	81.09
18	10.11	81.09	91.20
19	11.12	91.20	102.32
20	12.23	102.32	114.55
21	13.45	114.55	128.00
22	14.80	128.00	142.81
23	16.28	142.81	159.09
24	17.91	159.09	176.99
25	∞	176.99	∞

Data formats:

The data are available in the following formats:

- ER-Mapper (sub-folder: er_mapper). The grids are stored in ER Mapper binary floating point raster grid format (IEEE 4 byte reals) with an associated header (.ers) file. These are the original data supplied by GA.
- ESRI grid (sub-folder: ESRI_grid). The data are stored as ESRI floating point grids, converted from the ER-Mapper grids by ABARES.
- GeoTiff image format (sub-folder: geotif_image). Geo-referenced TIFF images of the AEM data using a pseudocolour colour stretch. Images include local hill-shading to emphasise subtle variation. The images were produced from the ER-Mapper grids by ABARES. Two colour stretches are provided:
    - 0-0.5 S/m (equivalent to 0-500 mS/m). Most suitable for viewing AEM conductivity data in the southern part of the AEM area.
    - 0-01.2 S/m (equivalent to 0-1200 mS/m). Most suitable for viewing AEM conductivity data in the northern part of the AEM area.

2.3 Depth slice grids (sub-folder: depth_slices)

The depth slice grids represent the average conductivity in S/m of various regular intervals (Table 2). They have been derived from the layer conductivity grids by a weighted average of the layers that intersect the depth interval. For example a slice between 5m and 10m depth would be constructed as follows:

$$\frac{(6.62-5)\times layer\ 3\ conductivity + (2.66)\times layer\ 4\ conductivity + (10-9.28)\times layer\ 5\ conductivity}{10-5}$$

.

Table 2 Depth slice intervals.

Depth to top (m)	Depth to bottom (m)	Thickness (m)
0	5	5
0	10	10
2	7	5
5	10	5
10	15	5
15	20	5
20	30	10
30	40	10
40	60	20
60	80	20
80	100	20
100	150	50
150	200	50

Data formats:

The data are available in the following formats:

- ER-Mapper (sub-folder: er_mapper). The grids are stored in ER Mapper binary floating point raster grid format (IEEE 4 byte reals) with an associated header (.ers) file. These are the original data supplied by GA.
- ESRI grid (sub-folder: ESRI_grid). The data are stored as ESRI floating point grids, converted from the ER-Mapper grids by ABARES.
- GeoTiff image format (sub-folder: geotif_image). Geo-referenced TIFF images of the AEM data using a pseudocolour colour stretch. Images include local hill-shading to emphasise subtle variation. The images were produced from the ER-Mapper grids by ABARES. Two colour stretches are provided:
    - 0-0.5 S/m (equivalent to 0-500 mS/m). Most suitable for viewing AEM conductivity data in the southern part of the AEM area.
    - 0-01.2 S/m (equivalent to 0-1200 mS/m). Most suitable for viewing AEM conductivity data in the northern part of the AEM area.

2.4 Vertical conductivity sections (sub-folder: sections)

The conductivity sections sub-folder contains a graphical conductivity depth colour section oriented along the line of best fit passing through the flight line. There is a separate Portable Document Format (.pdf) file for each flight line. To allow for the large range of conductivities encountered in the survey area, three different colour lookup tables were produced on each plot, namely: 0-0.5 S/m linear stretch, 0-1.2 S/m linear stretch, 0.01-1.0 S/m loag10 stretch.

Accompanying the conductivity sections are a range of graphs of parameters and diagnostics of the AEM inversion process.

2.5 AEM survey outline and flight line vector GIS data (sub-folder: survey_plan).

This directory contains ESRI shapefile GIS data of:

- the outline of the Lower Macquarie River TEMPEST AEM survey area and
- the actual flight line path flown in the survey, as a line dataset.

See Appendix 1 for details.

2.6 Borehole comparison logs (sub-folder: borehole_plots)

These plot the profile by depth of independent measurements of conductivity acquired down boreholes against the AEM inverted conductivity. These are available for each of the 83 bores inside the survey area for which downhole conductivity logs were acquired.

For each borehole the downhole log (black line) and the inverted conductivity profile (red line) is plotted in a JPG file. Because of the large line spacing in some places, the AEM data values are taken from the interpolated grids of the layer conductivities, rather than the nearest AEM sample to the borehole from the point located data.

3.0 DEM data

A digital elevation model (DEM) was acquired and processed by Fugro as part of the AEM survey acquisition process. The ground elevation was obtained by subtracting the terrain clearance from the aircraft laser altimeter from the aircraft elevation from differential GPS. The data was post processed using a de-corrugation filter. Details of the survey operations are provided in Noteboom and Stenning (2008).

The DEM is available as two parts: the southern flight zone (north-south oriented flight lines) and the northern flight zone (east-west flight lines).

The data are available in the following formats:

- ER-Mapper (sub-folder: er_mapper). The grids are stored in ER Mapper binary floating point raster grid format (IEEE 4 byte reals) with an associated header (.ers) file. These are the original data supplied by GA from Fugro.
- ESRI grid (sub-folder: ESRI_grid). The data are stored as ESRI floating point grids, converted from the ER-Mapper grids by ABARES.

4.0 Magnetics data

Magnetics data were acquired and processed by Fugro as part of the AEM survey acquisition process. The data are available as total magnetic intensity gridded data. Details of the survey operations are provided in Noteboom and Stenning (2008).

The Magnetics data are available as two parts: the southern flight zone (north-south oriented flight lines) and the northern flight zone (east-west flight lines).

The data are available in the following formats:

- ER-Mapper (sub-folder: er_mapper). The grids are stored in ER Mapper binary floating point raster grid format (IEEE 4 byte reals) with an associated header (.ers) file. These are the original data supplied by GA from Fugro.
- ESRI grid (sub-folder: ESRI_grid). The data are stored as ESRI floating point grids, converted from the ER-Mapper grids by ABARES.

5.0 Reports

This dataset includes the following reports:

Filename Lower_Macquarie_River_Report.pdf

Description Fugro Airborne Services (FAS) acquisition and processing report, Adobe Acrobat (PDF) format. This report summarises the procedures and equipment used by FAS in the acquisition, verification and processing of the airborne geophysical data.

Reference Noteboom, M., and Stenning, L., 2008. Lower Macquarie River Airborne Electromagnetic Mapping Survey Acquisition and Processing Report. Fugro Airborne Surveys, Floreat. WA.

Filename LMR_GA_AEM_InversionReport.pdf

Description AEM Inversion report from Geoscience Australia, Adobe Acrobat (PDF) format.

This report describes the geophysical inversion of the Lower Macquarie River TEMPEST airborne electromagnetic (AEM) survey data to produce subsurface electrical conductivity predictions using a layered earth inversion algorithm developed by Geoscience Australia (GA-LEI).

Reference Brodie, R. C., and Fisher, A., 2008. Inversion of Tempest AEM survey data, Lower Macquarie River, New South Wales. Geoscience Australia report to the Bureau of Rural Sciences.

Appendix 1 gives a detailed list of the contents of each directory and the dataset components.

Appendix 1. Details of the accompanying dataset

Directory	File name	File description
aem_data\borehole_plots	*.jpg	Comparison plots between downhole conductivity log data (black line) and AEM GA-LEI inversion data (red line). Images in JPEG format. One file image for each bore for which downhole conductivity logs were acquired in the survey area.
aem_data\depth_slices\er-mapper	depthslice_000m_005m.ers	75 m grid of conductivity in the 0 to 5 m depth slice produced by the GA-LEI.
	depthslice_000m_010m.ers	75 m grid of conductivity in the 0 to 10 m depth slice image produced by the GA-LEI.
	depthslice_000m_100m.ers	75 m grid of conductivity in the 0 to 100 m depth slice produced by the GA-LEI.
	depthslice_002m_007m.ers	75 m grid of conductivity in the 2 to 7 m depth slice produced by the GA-LEI.
	depthslice_005m_010m.ers	75 m grid of conductivity in the 5 to 10 m depth slice produced by the GA-LEI.
	depthslice_010m_015m.ers	75 m grid of conductivity in the 10 to 15 m depth slice produced by the GA-LEI.
	depthslice_015m_020m.ers	75 m grid of conductivity in the 15 to 20 m depth slice produced by the GA-LEI.
	depthslice_020m_030m.ers	75 m grid of conductivity in the 20 to 30 m depth slice produced by the GA-LEI.
	depthslice_030m_040m.ers	75 m grid of conductivity in the 30 to 40 m depth slice produced by the GA-LEI.
	depthslice_040m_060m.ers	75 m grid of conductivity in the 40 to 60 m depth slice produced by the GA-LEI.
	depthslice_060m_080m.ers	75 m grid of conductivity in the 60 to 80 m depth slice produced by the GA-LEI.
	depthslice_080m_100m.ers	75 m grid of conductivity in the 80 to 100 m depth slice produced by the GA-LEI.
	depthslice_100m_150m.ers	75 m grid of conductivity in the 100 to 150 m depth slice produced by the GA-LEI.
	depthslice_150m_200m.ers	75 m grid of conductivity in the 150 to 200 m depth slice produced by the GA-LEI.
aem_data\depth_slices\ersi_grid	ds_000_005	75 m grid of conductivity in the 0 to 5 m depth slice produced by the GA-LEI.
	ds_000_010	75 m grid of conductivity in the 0 to 10 m depth slice produced by the GA-LEI.
	ds_000_100	75 m grid of conductivity in the 0 to 100 m depth slice produced by the GA-LEI.
	ds_002_007	75 m grid of conductivity in the 2 to 7 m depth slice produced by the GA-LEI.
	ds_005_010	75 m grid of conductivity in the 5 to 10 m depth slice produced by the GA-LEI.
	ds_010_015	75 m grid of conductivity in the 10 to 15 m depth slice produced by the GA-LEI.
	ds_015_020	75 m grid of conductivity in the 15 to 20 m depth slice produced by the GA-LEI.
	ds_020_030	75 m grid of conductivity in the 20 to 30 m depth slice produced by the GA-LEI.
	ds_030_040	75 m grid of conductivity in the 30 to 40 m depth slice produced by the GA-LEI.
	ds_040_060	75 m grid of conductivity in the 40 to 60 m depth slice produced by the GA-LEI.
	ds_060_080	75 m grid of conductivity in the 60 to 80 m depth slice produced by the GA-LEI.
	ds_080_100	75 m grid of conductivity in the 80 to 100 m depth slice produced by the GA-LEI.
	ds_100_150	75 m grid of conductivity in the 100 to 150 m depth slice produced by the GA-LEI.
	ds_150_200	75 m grid of conductivity in the 150 to 200 m depth slice produced by the GA-LEI.
aem_data\depth_slices\geotif_image\ 0_500_mSm_stretch		AEM depth slice images using a 0-0.5 S/m (equivalent to 0-500 mS/m) pseudocolour colour stretch. Images include local hill-shading to emphasise subtle variation. Most suitable for viewing AEM conductivity data in the southern part of the AEM area.
	conductivity_legend_horizontal_500mSm.png	Legend image for 0-0.5 S/m stretch, horizontal format. Shows the correspondence betwen colours in the images below, and the corresponding AEM conductivity value.
	conductivity_legend_vertical_500mSm.png	As above, vertical format.

Directory	File name	File description
	depth_slice_000m_005m.tif	0 to 5 m depth slice image.
	depth_slice_005m_010m.tif	5 to 10 m depth slice image.
	depth_slice_010m_015m.tif	10 to 15 m depth slice image.
	depth_slice_015m_020m.tif	15 to 20 m depth slice image.
	depth_slice_020m_030m.tif	20 to 30 m depth slice image.
	depth_slice_030m_040m.tif	30 to 40 m depth slice image.
	depth_slice_040m_060m.tif	40 to 60 m depth slice image.
	depth_slice_060m_080m.tif	60 to 80 m depth slice image.
	depth_slice_080m_100m.tif	80 to 100 m depth slice image.
	depth_slice_100m_150m.tif	100 to 150 m depth slice image.
	depth_slice_150m_200m.tif	150 to 200 m depth slice image.
aem_data\depth_slices\geotif_image\ 0_1200_mSm_stretch		AEM depth slice images using a 0-01.2 S/m (equivalent to 0-1200 mS/m) pseudocolour colour stretch. Images include local hill-shading to emphasise subtle variation. Most suitable for viewing AEM conductivity data in the northern part of the AEM area.
	conductivity_legend_horizontal_1200mSm.png	Legend image for 0-1.2 S/m stretch, horizontal format. Shows the correspondence between colours in the images below, and the corresponding AEM conductivity value.
	conductivity_legend_vertical_1200mSm.png	As above, vertical format.
	depth_slice_000m_005m.tif	0 to 5 m depth slice image.
	depth_slice_005m_010m.tif	5 to 10 m depth slice image.
	depth_slice_010m_015m.tif	10 to 15 m depth slice image.
	depth_slice_015m_020m.tif	15 to 20 m depth slice image.
	depth_slice_020m_030m.tif	20 to 30 m depth slice image.
	depth_slice_030m_040m.tif	30 to 40 m depth slice image.
	depth_slice_040m_060m.tif	40 to 60 m depth slice image.
	depth_slice_060m_080m.tif	60 to 80 m depth slice image.
	depth_slice_080m_100m.tif	80 to 100 m depth slice image.
	depth_slice_100m_150m.tif	100 to 150 m depth slice image.
	depth_slice_150m_200m.tif	150 to 200 m depth slice image.
aem_data\inversion_layers\er-mapper	lev_conductivity_01.ers	75 m grid of conductivity for layer 1 (0.00-2.00 m) produced by the GA-LEI
	lev_conductivity_02.ers	75 m grid of conductivity for layer 2 (2.00-4.20 m) produced by the GA-LEI
	lev_conductivity_03.ers	75 m grid of conductivity for layer 3 (4.20-6.62 m) produced by the GA-LEI
	lev_conductivity_04.ers	75 m grid of conductivity for layer 4 (6.62-9.28 m) produced by the GA-LEI
	lev_conductivity_05.ers	75 m grid of conductivity for layer 5 (9.28-12.21 m) produced by the GA-LEI
	lev_conductivity_06.ers	75 m grid of conductivity for layer 6 (12.21-15.43 m) produced by the GA-LEI
	lev_conductivity_07.ers	75 m grid of conductivity for layer 7 (15.43-18.97 m) produced by the GA-LEI
	lev_conductivity_08.ers	75 m grid of conductivity for layer 8 (18.97-22.87 m) produced by the GA-LEI
	lev_conductivity_09.ers	75 m grid of conductivity for layer 9 (22.87-27.16 m) produced by the GA-LEI
	lev_conductivity_10.ers	75 m grid of conductivity for layer 10 (27.16-31.87 m) produced by the GA-LEI
	lev_conductivity_11.ers	75 m grid of conductivity for layer 11 (31.87-37.06 m) produced by the GA-LEI
	lev_conductivity_12.ers	75 m grid of conductivity for layer 12 (37.06-42.77 m) produced by the GA-LEI

Directory	File name	File description
	lev_conductivity_13.ers	75 m grid of conductivity for layer 13 (42.77-49.05 m) produced by the GA-LEI
	lev_conductivity_14.ers	75 m grid of conductivity for layer 14 (49.05-55.95 m) produced by the GA-LEI
	lev_conductivity_15.ers	75 m grid of conductivity for layer 15 (55.95-63.54 m) produced by the GA-LEI
	lev_conductivity_16.ers	75 m grid of conductivity for layer 16 (63.54-71.90 m) produced by the GA-LEI
	lev_conductivity_17.ers	75 m grid of conductivity for layer 17 (71.90-81.09 m) produced by the GA-LEI
	lev_conductivity_18.ers	75 m grid of conductivity for layer 18 (81.09-91.20 m) produced by the GA-LEI
	lev_conductivity_19.ers	75 m grid of conductivity for layer 19 (91.20-102.32 m) produced by the GA-LEI
	lev_conductivity_20.ers	75 m grid of conductivity for layer 20 (102.32-114.55 m) produced by the GA-LEI
	lev_conductivity_21.ers	75 m grid of conductivity for layer 21 (114.55-128.00 m) produced by the GA-LEI
	lev_conductivity_22.ers	75 m grid of conductivity for layer 22 (128.00-142.81 m) produced by the GA-LEI
	lev_conductivity_23.ers	75 m grid of conductivity for layer 23 (142.81-159.09 m) produced by the GA-LEI
	lev_conductivity_24.ers	75 m grid of conductivity for layer 24 (159.09-176.99 m) produced by the GA-LEI
	lev_conductivity_25.ers	75 m grid of conductivity for layer 25 (176.99-∞ m) produced by the GA-LEI
aem_data\inversion_layers\ersi_grid	lev_layer_01	75 m grid of conductivity for layer 1 (0.00-2.00 m) produced by the GA-LEI
	lev_layer_02	75 m grid of conductivity for layer 2 (2.00-4.20 m) produced by the GA-LEI
	lev_layer_03	75 m grid of conductivity for layer 3 (4.20-6.62 m) produced by the GA-LEI
	lev_layer_04	75 m grid of conductivity for layer 4 (6.62-9.28 m) produced by the GA-LEI
	lev_layer_05	75 m grid of conductivity for layer 5 (9.28-12.21 m) produced by the GA-LEI
	lev_layer_06	75 m grid of conductivity for layer 6 (12.21-15.43 m) produced by the GA-LEI
	lev_layer_07	75 m grid of conductivity for layer 7 (15.43-18.97 m) produced by the GA-LEI
	lev_layer_08	75 m grid of conductivity for layer 8 (18.97-22.87 m) produced by the GA-LEI
	lev_layer_09	75 m grid of conductivity for layer 9 (22.87-27.16 m) produced by the GA-LEI
	lev_layer_10	75 m grid of conductivity for layer 10 (27.16-31.87 m) produced by the GA-LEI
	lev_layer_11	75 m grid of conductivity for layer 11 (31.87-37.06 m) produced by the GA-LEI
	lev_layer_12	75 m grid of conductivity for layer 12 (37.06-42.77 m) produced by the GA-LEI
	lev_layer_13	75 m grid of conductivity for layer 13 (42.77-49.05 m) produced by the GA-LEI
	lev_layer_14	75 m grid of conductivity for layer 14 (49.05-55.95 m) produced by the GA-LEI
	lev_layer_15	75 m grid of conductivity for layer 15 (55.95-63.54 m) produced by the GA-LEI
	lev_layer_16	75 m grid of conductivity for layer 16 (63.54-71.90 m) produced by the GA-LEI
	lev_layer_17	75 m grid of conductivity for layer 17 (71.90-81.09 m) produced by the GA-LEI
	lev_layer_18	75 m grid of conductivity for layer 18 (81.09-91.20 m) produced by the GA-LEI
	lev_layer_19	75 m grid of conductivity for layer 19 (91.20-102.32 m) produced by the GA-LEI
	lev_layer_20	75 m grid of conductivity for layer 20 (102.32-114.55 m) produced by the GA-LEI
	lev_layer_21	75 m grid of conductivity for layer 21 (114.55-128.00 m) produced by the GA-LEI
	lev_layer_22	75 m grid of conductivity for layer 22 (128.00-142.81 m) produced by the GA-LEI
	lev_layer_23	75 m grid of conductivity for layer 23 (142.81-159.09 m) produced by the GA-LEI
	lev_layer_24	75 m grid of conductivity for layer 24 (159.09-176.99 m) produced by the GA-LEI
	lev_layer_25	75 m grid of conductivity for layer 25 (176.99-∞ m) produced by the GA-LEI
aem_data\inversion_layers\geotif_image\0_500_mSm_stretch	lev_conductivity_01.tif	Image of 75 m grid of 0 to 500mSm conductivity for layer 1 (0.00-2.00 m)
	lev_conductivity_02.tif	Image of 75 m grid of 0 to 500mSm conductivity for layer 2 (2.00-4.20 m)
	lev_conductivity_03.tif	Image of 75 m grid of 0 to 500mSm conductivity for layer 3 (4.20-6.62 m)
	lev_conductivity_04.tif	Image of 75 m grid of 0 to 500mSm conductivity for layer 4 (6.62-9.28 m)

Directory	File name	File description
	lev_conductivity_05.tif	Image of 75 m grid of 0 to 500mSm conductivity for layer 5 (9.28-12.21 m)
	lev_conductivity_06.tif	Image of 75 m grid of 0 to 500mSm conductivity for layer 6 (12.21-15.43 m)
	lev_conductivity_07.tif	Image of 75 m grid of 0 to 500mSm conductivity for layer 7 (15.43-18.97 m)
	lev_conductivity_08.tif	Image of 75 m grid of 0 to 500mSm conductivity for layer 8 (18.97-22.87 m)
	lev_conductivity_09.tif	Image of 75 m grid of 0 to 500mSm conductivity for layer 9 (22.87-27.16 m)
	lev_conductivity_10.tif	Image of 75 m grid of 0 to 500mSm conductivity for layer 10 (27.16-31.87 m)
	lev_conductivity_11.tif	Image of 75 m grid of 0 to 500mSm conductivity for layer 11 (31.87-37.06 m)
	lev_conductivity_12.tif	Image of 75 m grid of 0 to 500mSm conductivity for layer 12 (37.06-42.77 m)
	lev_conductivity_13.tif	Image of 75 m grid of 0 to 500mSm conductivity for layer 13 (42.77-49.05 m)
	lev_conductivity_14.tif	Image of 75 m grid of 0 to 500mSm conductivity for layer 14 (49.05-55.95 m)
	lev_conductivity_15.tif	Image of 75 m grid of 0 to 500mSm conductivity for layer 15 (55.95-63.54 m)
	lev_conductivity_16.tif	Image of 75 m grid of 0 to 500mSm conductivity for layer 16 (63.54-71.90 m)
	lev_conductivity_17.tif	Image of 75 m grid of 0 to 500mSm conductivity for layer 17 (71.90-81.09 m)
	lev_conductivity_18.tif	Image of 75 m grid of 0 to 500mSm conductivity for layer 18 (81.09-91.20 m)
	lev_conductivity_19.tif	Image of 75 m grid of 0 to 500mSm conductivity for layer 19 (91.20-102.32 m)
	lev_conductivity_20.tif	Image of 75 m grid of 0 to 500mSm conductivity for layer 20 (102.32-114.55 m)
	lev_conductivity_21.tif	Image of 75 m grid of 0 to 500mSm conductivity for layer 21 (114.55-128.00 m)
	lev_conductivity_22.tif	Image of 75 m grid of 0 to 500mSm conductivity for layer 22 (128.00-142.81 m)
	lev_conductivity_23.tif	Image of 75 m grid of 0 to 500mSm conductivity for layer 23 (142.81-159.09 m)
	lev_conductivity_24.tif	Image of 75 m grid of 0 to 500mSm conductivity for layer 24 (159.09-176.99 m)
	lev_conductivity_25.tif	Image of 75 m grid of 0 to 500mSm conductivity for layer 25 (176.99-∞ m)
aem_data\inversion_layers\geotif_image\0_1200_mSm_stretch	lev_conductivity_01.tif	Image of 75 m grid of 0 to 1200mSm conductivity for layer 1 (0.00-2.00 m)
	lev_conductivity_02.tif	Image of 75 m grid of 0 to 1200mSm conductivity for layer 2 (2.00-4.20 m)
	lev_conductivity_03.tif	Image of 75 m grid of 0 to 1200mSm conductivity for layer 3 (4.20-6.62 m)
	lev_conductivity_04.tif	Image of 75 m grid of 0 to 1200mSm conductivity for layer 4 (6.62-9.28 m)
	lev_conductivity_05.tif	Image of 75 m grid of 0 to 1200mSm conductivity for layer 5 (9.28-12.21 m)
	lev_conductivity_06.tif	Image of 75 m grid of 0 to 1200mSm conductivity for layer 6 (12.21-15.43 m)
	lev_conductivity_07.tif	Image of 75 m grid of 0 to 1200mSm conductivity for layer 7 (15.43-18.97 m)
	lev_conductivity_08.tif	Image of 75 m grid of 0 to 1200mSm conductivity for layer 8 (18.97-22.87 m)
	lev_conductivity_09.tif	Image of 75 m grid of 0 to 1200mSm conductivity for layer 9 (22.87-27.16 m)
	lev_conductivity_10.tif	Image of 75 m grid of 0 to 1200mSm conductivity for layer 10 (27.16-31.87 m)
	lev_conductivity_11.tif	Image of 75 m grid of 0 to 1200mSm conductivity for layer 11 (31.87-37.06 m)
	lev_conductivity_12.tif	Image of 75 m grid of 0 to 1200mSm conductivity for layer 12 (37.06-42.77 m)
	lev_conductivity_13.tif	Image of 75 m grid of 0 to 1200mSm conductivity for layer 13 (42.77-49.05 m)
	lev_conductivity_14.tif	Image of 75 m grid of 0 to 1200mSm conductivity for layer 14 (49.05-55.95 m)
	lev_conductivity_15.tif	Image of 75 m grid of 0 to 1200mSm conductivity for layer 15 (55.95-63.54 m)
	lev_conductivity_16.tif	Image of 75 m grid of 0 to 1200mSm conductivity for layer 16 (63.54-71.90 m)
	lev_conductivity_17.tif	Image of 75 m grid of 0 to 1200mSm conductivity for layer 17 (71.90-81.09 m)
	lev_conductivity_18.tif	Image of 75 m grid of 0 to 1200mSm conductivity for layer 18 (81.09-91.20 m)
	lev_conductivity_19.tif	Image of 75 m grid of 0 to 1200mSm conductivity for layer 19 (91.20-102.32 m)
	lev_conductivity_20.tif	Image of 75 m grid of 0 to 1200mSm conductivity for layer 20 (102.32-114.55 m)
	lev_conductivity_21.tif	Image of 75 m grid of 0 to 1200mSm conductivity for layer 21 (114.55-128.00 m)

Directory	File name	File description
	lev_conductivity_22.tif	Image of 75 m grid of 0 to 1200mSm conductivity for layer 22 (128.00-142.81 m)
	lev_conductivity_23.tif	Image of 75 m grid of 0 to 1200mSm conductivity for layer 23 (142.81-159.09 m)
	lev_conductivity_24.tif	Image of 75 m grid of 0 to 1200mSm conductivity for layer 24 (159.09-176.99 m)
	lev_conductivity_25.tif	Image of 75 m grid of 0 to 1200mSm conductivity for layer 25 (176.99-∞ m)
aem_data\line_data		Line (point located) data of layer conductivity, depths below ground level, and thicknesses. These are the primary data output of the GA-LEI inversion process
aem_data\line_data\levelled	inversion.output.levelled.dat	Levelled final point located AEM data produced by the GA-LEI (see .hdr file for details)
aem_data\line_data\unlevelled	inversion.output.dat	Final point located AEM data produced by the GA-LEI (see .hdr file for details)
aem_data\sections	*.pdf	Conductivity-depth sections along flight lines. These are graphical representations of the estimated conductivity in a vertical slice along the line of best fit passing through the flight line. These sections were produced for each flight line in the AEM survey.
aem_data\survey_plan\survey_area_shapefiles	lmr_surveyarea_north_final.shp	Shapefile of the outline of the north block of the AEM survey area.
	lmr_surveyarea_outline_final.shp	Shapefile of the outline of the AEM survey area, both north and south, as a single outline. Does not include the overlap between the two zones.
	lmr_surveyarea_south_final.shp	Shapefile of the outline of the south block of the AEM survey area.
	lmr_surveyareas_spacingzones_final.shp	Shapefile showing outlining the various flight line spacing blocks that comprise the AEM survey area. Attribute "line_space" gives the line spacing, "direction" gives the flight line orientation (East-West of North-South).
aem_data\survey_plan\survey_lines_shapefiles	survey_lines_north.shp	ESRI shape files of the flight lines of the AEM survey area, north. Attribute "linenum" gives the flight line number for each line. Note: there is an overlap between the north and south zones.
	survey_lines_south.shp	ESRI shape files of the flight lines of the AEM survey area, south. Attribute "linenum" gives the flight line number for each line.
dem_data\er-mapper	dem124m_278m_linearStretch.alg	ER-Mapper algorithm image of the digital elevation model (DEM) 124 – 278 m linear stretch
	north_dtm.ers	DEM for the north flight area.
	south_dtm.ers	DEM for the south flight area.
dem_data\esri_grid	north_dtm	DEM for the north flight area.
	south_dtm	DEM for the south flight area.
mag_data\er-mapper	north_mag.ers	Total Magnetic Intensity grid for the north flight area.
	south_mag.ers	Total Magnetic Intensity grid for the south flight area.
mag_data\esri_grid	north_mag	Total Magnetic Intensity grid for the north flight area.
	south_mag	Total Magnetic Intensity grid for the south flight area.

Directory	File name	File description
reports	citation_list.pdf	PDF document describing the reports in this directory and their citation references.
	LMR_Fugro_AEMAcquisitionReport.pdf	PDF file of the Fugro Airborne Services (FAS) acquisition and processing report. This report summarises the procedures and equipment used by FAS in the acquisition, verification and processing of the airborne geophysical data.
	LMR_GA_AEMInversionReport.pdf	PDF file of AEM Inversion report from Geoscience Australia. This report describes the geophysical inversion of the Lower Macquarie River TEMPEST airborne electromagnetic (AEM) survey data to produce subsurface electrical conductivity predictions using a layered earth inversion algorithm developed by Geoscience Australia (GA-LEI).

Notes:

- All grids (ER-Mapper and ESRI Grids), images (.tif & .jpg) and shapefiles (.shp) are located in the Geodetic Datum of Australia, Map Grid of Australia Zone 55 coordinate system.

- The tif and jpg images can be viewed in many software packages, and they also have associated world files (.tfw and .jgw) and projection files (.xml) that contain spatial reference information for viewing in GIS software, such as ESRI ArcGIS.

- To view ER-Mapper grids (.ers format) and ER-Mapper algorithm images (.alg), you will need to download the ER Mapper Plugin appropriate to your GIS system. These are available for free download from: http://www.erdas.com

- The above GIS data have been tested using ESRI ArcGIS ArcMap version 9.2, with the ER Mapper plugin "ArcGIS 8.x and 9.x ECW JPEG 2000 plugin" version 4.2.